Bioresource Technology 391 (2024) 129935

Contents lists available at ScienceDirect

Bioresource Technology

journal homepage: www.elsevier.com/locate/biortech

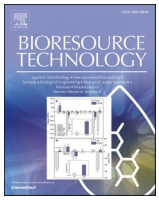

Engineered co-culture for consolidated production of phenylpropanoids directly from aromatic-rich biomass

Micaela Chacón [a], Ellen Percival [b], Timothy D.H. Bugg [b], Neil Dixon [a,*]

[a] Manchester Institute of Biotechnology (MIB), Department of Chemistry, University of Manchester, Manchester M1 7DN, UK
[b] Department of Chemistry, University of Warwick, Coventry CV4 7AK, UK

GRAPHICAL ABSTRACT

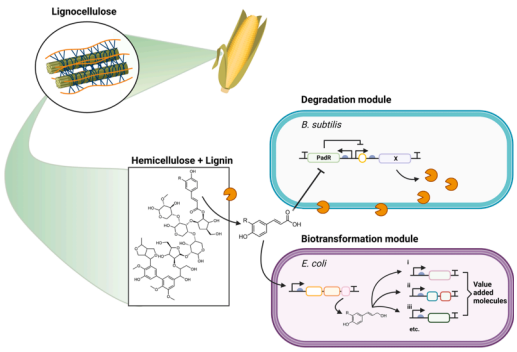

ARTICLE INFO

Keywords:
Corncob lignocellulose
Hydroxycinnamic acids
Co-culture
Protein secretion
Biotransformation

ABSTRACT

Consolidated bioprocesses for the *in situ* hydrolysis and conversion of biomass feedstocks into value-added products offers great potential for both process and cost reduction. However, to date few consolidated bioprocesses have been developed that target aromatic rich feedstock fractions. Reported here is the development of synthetic co-cultivation for the consolidated hydrolysis and valorisation of corncob hydroxycinnamic acids. Biomass hydrolysis was achieved via a secretion module developed in *B. subtilis* using a genetically encoded biosensor-actuator to secrete hydrolytic enzymes. Conversion was achieved via a biotransformation module developed in *E. coli* using a suite of plug-and-play encoded enzymes to convert the released hydroxycinnamic acids into high-value phenylpropanoid target compounds. Finally, employing cellulolytic pre-treatment, extractive fermentation and *in situ* product recovery multiple aromatic products, coniferol and chavicol, were isolated from the same process in high purity.

1. Introduction

Lignocellulosic biomass is a renewable and abundant feedstock with potential to replace the petroleum resources predominantly employed in the production of a number of fuels, solvents and commodity chemicals (Schmitz et al., 2022; Zoghlami and Paës, 2019). Microbial

* Corresponding author.
E-mail address: neil.dixon@manchester.ac.uk (N. Dixon).

https://doi.org/10.1016/j.biortech.2023.129935
Received 26 September 2023; Received in revised form 26 October 2023; Accepted 26 October 2023
Available online 2 November 2023

bioconversion of lignocellulose is multi step, involving the production of lignocellulolytic enzymes, hydrolysis of the biomass feedstock to monomeric units, and the uptake and utilisation of the released monomers by a microbial host for growth and/or production. Despite the promise of the biorefinery concept, it is still challenged by low conversion efficiency and high process costs (Singhania et al., 2022). As such, economic motivation has spurred research into the development of consolidated bioprocesses (CBP), whereby all biologically mediated transformation steps are integrated into a single unit operation, thereby reducing the operating/capital costs and potentially improving process efficiency by providing a thermodynamic sink for released sugars. Typically, CBP involves use of a single microorganism, engineered to simultaneously carry out the two core functionalities of (1) secretion of hydrolytic enzymes for feedstock deconstruction and (2) conversion the released monomers into a target product. The majority of this research has focused on the hydrolysis and use of the carbohydrate fraction of lignocellulose for the production of endogenous fermentation products (Mazzoli, 2021).

A drawback to traditional CBP is the inherent challenge of engineering and optimising single strains to perform multiple complex functions. This lack of specialisation results in hosts being required to divide metabolic resources between multiple functions, e.g., secretion and production of the target products. Such competition scenarios result in excessive demand upon the host, negatively impacting growth and productivity (Minty et al., 2013). In nature, microbes typically live in synergistic consortia whereby individuals occupy specialised roles and cooperate with one another in order to complete complex functions together. Inspired by the success of natural microbial communities, there is great interest in engineering synthetic consortia for biotechnology applications. In contrast to the "superbug" model of CBP, growing evidence suggests that distributing discrete objectives across subpopulations in a co-culture can improve overall performance by virtue of expanded machinery/resource availability and reduced metabolic burden on each constituent strain (Zhang and Wang 2016). With co-culture CBP, typically, a dividing line is drawn between the labour of hydrolytic enzyme secretion and the labour of end-product formation, with each task being allocated to a specialist(s). CBP using synthetic co-cultures has been successfully demonstrated for the production of a number of bulk chemicals from the carbohydrate fraction of lignocellulosic feedstocks (Liu et al., 2019; Shahab et al., 2018; Minty et al., 2013).

Unlike the carbohydrate fraction of lignocellulose, little work has been done towards expanding the CBP concept towards the aromatic fraction. Notably, however, Salvachúa et al., (2015) evaluated the ability of a number of bacteria to perform monoculture lignin-centric CBP and utilise the released aromatics in combination with sugars and acids to produce polyhydroxyalkanoates (PHAs) and fatty acid methyl esters (FAMEs). The aromatic content of lignocellulose can range between 15 and 30 %, comprising both the lignin heteropolymer and the hemicellulose fractions. Many of the aromatic species within these fractions possess potential as starting materials for the production of fuels or fine and specialty chemicals (Sethupathy et al., 2022; Tramontina et al., 2020; Alvarez-Gonzalez and Dixon, 2019; Rinaldi et al., 2016). The technical challenge posed by the lignin fraction of lignocellulose stems from the heterogeneity of its constituent monomers and the variety of chemical bond types cross-linking them within the matrix, both of which contribute to its recalcitrance to degradation. Two of the most abundant aromatic constituents of lignocellulose are ferulic acid (FA) and coumaric acid (CA), which play a role in crosslinking the lignin and hemicellulose fractions via ether or ester linkages respectively. In grasses especially these hydroxycinnamic acids are abundant and can represent up to 3.1 % of the dry weight of the cell wall (Buanafina, 2009). Both FA and CA have direct value as antioxidants or can be used as building blocks for the production of pharmaceuticals, polymers, and flavour/fragrance molecules. A number of these commercially valuable derivatives can be sustainably achieved via microbial transformation (Galman et al., 2022; Wang et al., 2019). Indeed, previously it was demonstrated that coniferol and coumarol can be produced directly from biomass residues following hydrolytic release and reduction of FA and CA (Tramontina et al., 2020). However, this previous study required additional processing steps to produce the required hydrolytic enzymes separately, and to purify the co-produced targets compounds. In addition to being high-value flavour and fragrance compounds, coniferol and coumarol can also in principle be further derivatised into other commercially relevant esters, ethers, allylphenols and propenylphenols. Chavicol, a phenylpropene derived from coumaric acid, has historically been extracted from non-traditional crops for use as an ingredient in odorants and perfumes. Industrial interest for its use in high performance thermoset resins, as an anti-inflammatory therapeutic precursor, antimicrobial, and flavour/fragrance ingredient has spurred interest in developing more sustainable routes for its production (Brooks et al., 2023; Dhar et al., 2020; Dumas et al., 2016).

High titre bio-production is often constrained by metabolic imbalance and burden. A successful strategy for improving production titres and strain robustness is the use of dynamic metabolic engineering, for which genetically encoded biosensors are a key tool. Biosensors detect the presence of certain effector molecules and transduce that signal in a dose dependent manner to regulate downstream genes encoding reporter proteins or biosynthetic machinery. A variety of such biosensors have been developed to detect lignocellulose derived sugars and aromatics, providing a valuable *in situ* diagnostic tool (Alvarez-Gonzalez and Dixon, 2019). Further, they have been employed for autonomous and dynamic induction of designer genetic circuits, permitting discrete control of gene expression in response to the presence of effector molecule, mimicking native metabolic control systems (Hartline et al., 2021). In the context of CBP, the use of biosensors can enable more dynamic metabolic interaction between constituent strains and the substrate and/or one another.

Despite the diverse commercial potential of the individual aromatic constituents of lignocellulose, to date the majority of microbial based aromatic valorisation research has focused on funnelling the heterogeneous mix of monomers released from the matrix – via either a thermochemical or enzymatic hydrolysis – into common end-products derived from central metabolism (Barton et al., 2018; Wei et al., 2015; Linger et al., 2014). Instead, this work demonstrates the development of a targeted hydroxycinnamic acid CBP strategy where the two biological functions, (i) enzyme mediated FA and CA release from lignocellulose and (ii) biotransformation of the released aromatic residues into desired end-products, are divided between two microbial specialists. The hydrolysis module was achieved by engineering *Bacillus subtilis* to secrete an optimal combination of enzymes for the release of ferulic and coumaric acid directly from milled corncob, while the biotransformation module was achieved by engineering a suite of plug-and-play *Escherichia coli* strains capable of producing a number of value-added FA and CA derivatives, including coniferyl/coumaryl (di)acetates, 4-*O*-coniferyl methyl ether, eugenol, isoeugenol, chavicol and chavicol acetate. A *B. subtilis*:*E.coli* co-culture was successfully demonstrated for the consolidated hydrolysis and bioconversion of lignocellulose linked FA and CA to coniferol and chavicol, respectively. *In situ* aqueous-organic phase separation during co-cultivation was used to segregate each end product for ease of downstream purification.

2. Materials and methods

2.1. Plasmid construction

All gene sequences and plasmid construction details can be found in Table 1 and see Supplementary Materials. All DNA synthesis and oligonucleotide primer synthesis was performed by Integrated DNA Technologies. All heterologously expressed genes were codon optimized to their respective expression host with the exception of SAAT, BEAT and the signal peptide sequence of XynZ. DNA amplification for cloning

Table 1
Plasmids and strains used in this study.

Name	Description	Reference/Source
Strains		
DH5α	*E. coli* Cloning strain	NEB
BL21(DE3)	*E. coli* Expression strain	Invitrogen
EC-*CAAT-mCh*	*E. coli* BL21(DE3) expressing plasmid pROB-CAAT-mCherry	This study
KO7	*B. subtilis* 168 Δ*nprE* Δ*aprE* Δ*epr* Δ*mpr* Δ*nrpB* Δ*vpr* Δ*bpr*	BGSC
BS01	*B. subtilis* KO7 Δ*PadC*::*PrsA*, *DnaK*	This study
BS01-*GFP*	BS01 expressing plasmid pC1622-PadR-GFP	This study
BS01-*CE1-GFP*	BS01 expressing plasmid pC1622-PadR-CE1-GFP	This study
BS01-*XynZ*	BS01 expressing plasmid pC1622-PadR-XynZ	This study
BS01-*XynZ-GFP*	BS01 expressing plasmid pC1622-PadR-GFP-XynZ	This study
Plasmid		
pET28a::CAT	pColE1, Kan^R, P_{T7}-CAT_{Ec}	This study
pET28a::CFAT	pColE1, Kan^R, P_{T7}-$CFAT_{Ph}$	This study
pET28a::CAAT	pColE1, Kan^R, P_{T7}-$CAAT_{Lt}$	This study
pET28a:: ObAAT	pColE1, Kan^R, P_{T7}-AAT_{Ob}	This study
pET151::SAAT	pColE1, Kan^R, P_{T7}-$SAAT_{Fa}$	This study
pET151::BEAT	pColE1, Kan^R, P_{T7}-$BEAT_{Cb}$	This study
pET28a::MOMT9	pColE1, Kan^R, P_{T7}-$MOMT9_{Cb}$	This study
pET28a::CFAT-PhEGS	pColE1, Kan^R, P_{T7}-$CFAT_{Ph}$-EGS_{Ph}	This study
pET28a:: CFAT-CbEGS	pColE1, Kan^R, P_{T7}- $CFAT_{Ph}$-EGS_{Cb}	This study
pET28a:: CFAT-ObEGS	pColE1, Kan^R, P_{T7}- $CFAT_{Ph}$-EGS_{Ob}	This study
pET28a:: CFAT-PhIGS	pColE1, Kan^R, P_{T7}- $CFAT_{Ph}$-IGS_{Ph}	This study
pET28a:: CFAT-CbIGS	pColE1, Kan^R, P_{T7}- $CFAT_{Ph}$-IGS_{Cb}	This study
pROB-CAT	pColE1, Kan^R, P_{proB}-AKR_{Cg}-$CAR5_{Ni}$-*sfp variant*- P_{veg}-CAT_{Ec}	This study
pROB-CAAT	pColE1, Kan^R, P_{proB}-AKR_{Cg}-$CAR5_{Ni}$-*sfp variant*- P_{veg}-$CAAT_{Lt}$	This study
pROB-CFAT	pColE1, Kan^R, P_{proB}-AKR_{Cg}-$CAR5_{Ni}$-*sfp variant*- P_{veg}-$CFAT_{Ph}$	This study
pROB-BEAT	pColE1, Kan^R, P_{proB}-AKR_{Cg}-$CAR5_{Ni}$-*sfp variant*- P_{veg}-$BEAT_{Cb}$	This study
pROB-CFAT-PhEGS	pColE1, Kan^R, P_{proB}-AKR_{Cg}-$CAR5_{Ni}$-*sfp variant*- P_{veg}- $CFAT_{Ph}$-EGS_{Ph}	This study
pROB-CFAT-CbIGS	pColE1, Kan^R, P_{proB}-AKR_{Cg}-$CAR5_{Ni}$-*sfp variant*- P_{veg}- $CFAT_{Ph}$-IGS_{Cb}	This study
pROB-MOMT9	pColE1, Kan^R, P_{proB}-AKR_{Cg}-$CAR5_{Ni}$-*sfp variant*- P_{veg}- $MOMT9_{Cb}$	This study
pROB-CAAT-mCherry	pColE1, Kan^R, P_{proB}-AKR_{Cg}-$CAR5_{Ni}$-*sfp variant*- P_{veg}-$CAAT_{Lt}$-*mCherry*	This study
pET151::Dyp1B	pColE1, Amp^R, P_{T7}-$Dyp1B_{Pf}$	Rahmanpour and Bugg, 2015
pET151::CopA	pColE1, Amp^R, P_{T7}-$CopA_{Pp}$	Granja-Travez and Bugg, 2018
pET151::CueO	pColE1, Amp^R, P_{T7}-$CueO_{Osp.}$	Granja-Travez et al., 2018
pDG1644-PadC::PrsA-DnaK	pColE1, Amp^R, *PadC*::P_{veg}-$PrsA_{Bs}$-$DnaK_{Bs}$-Kan^R	This study
pC1622-PadR-GFP	pBC16, Kan^R, P_{xylR}-$PadR_{Bs}$-P_{veg}-*sfGFP*	This study
pC1622-PadR-CE1-GFP	pBC16, Kan^R, P_{xylR}-$PadR_{Bs}$-P_{veg}-$CE1_{Ct}$-*sfGFP*	This study
pC1622-PadR-XynZ	pBC16, Kan^R, P_{xylR}-$PadR_{Bs}$-P_{veg}-$XynZ_{Ct}$	This study
pC1622-PadR-GFP-XynZ	pBC16, Kan^R, P_{xylR}-$PadR_{Bs}$-*sfGFP*-P_{veg}-$XynZ_{Ct}$	This study

Ec = *Escherichia coli*, Ph = *Petunia hybrida*, Lt = *Larrea tridentata*, Ob = *Ocimum basilicum*, Fa = *F.* × *ananassa* cv. Elsanta, Cb = *Clarkia breweri*, Cg = *Coptotermes gestroi*, Ni = *Nocardia Iowensis*, Pf = *Pseudomonas fluorescens*, Pp = *Pseudomonas putida*, Osp. = *Ochrobatrum* sp. Bs = *Bacillus subtilis*, Ct = *Clostridia thermocellum*.

was performed using Q5 Hot Start High-Fidelity 2x Master Mix (NEB), and DNA amplification for colony PCR was performed using Phire Green Hot Start II Master Mix (Thermo Fisher Scientific). Plasmid assembly was performed using NEBuilder HiFi DNA Assembly Master Mix (NEB) followed by transformation into NEB 5-alpha competent *E. coli* cells. Validation of correct plasmid assembly was done using Sanger sequencing (Eurofins Genomic, Germany).

2.2. *B. subtilis* genome modification

The genomic knock-out/knock-in of strain BS01 was performed using the standard Spizizen protocol. Briefly, chemically competent *B. subtilis* KO7 cells were transformed with 1 μg of linearised pDG1664 plasmid harbouring the relevant *padC* homology arms and *prsA* and *danK* gene inserts (see Supplementary Materials), plated onto LB + Kan (10 g/L tryptone, 10 g/l NaCl, 5 g/L yeast extract, 15 g/L agar and 5 mg/mL) and incubated at 37 °C. Successful knock-out/knock-ins were validated by cPCR and Sanger sequencing.

2.3. Assay of hydroxycinnamic acid release from corncob

Proteins Dyp1B, CopA and CueO were produced and purified from *E. coli* BL21(DE3) according to Rahmanpour and Bugg, (2015), Granja-Travez and Bugg (2018), and Granja-Travez et al. (2018), respectively. CE1 from *C. thermocellum* and α-Gluc (GH67) from *Cellvibrio japonicas* were purchased from Prozomix (UK), while Xyl (GH11) from an unspecified rumen microorganism and AraF (GH51) from *Aspergillus niger* were purchased from Megazyme (UK). Assays were performed at 10 % solid loading (w/w) in 100 mM phosphate buffer pH 7.0 in 20 mL vials at 37 °C and 150 rpm. Corncob slurry was incubated at 37 °C for 1 h prior to the addition of 1 mg protein/g corncob for each respective protein in a given condition. Hydrolysate was harvested at 24 h for quantification of aromatic acid release, samples were passed through a 0.22 μm filter before being stored at −20 °C.

2.4. *B. subtilis* cultivation

Precultures of *B. subtilis* KO7 and BS01 were grown overnight in LB at 37 ℃ used to inoculate 50 mL of LB media +/- ferulic or coumaric acid to an OD_{600} of 0.05, in triplicate. Cultures were incubated at 37 ℃ and 180 rpm with intermittent samples taken to determine culture density (OD_{600}) and substrate conversion. For the latter analysis, 1 mL of culture was centrifuged at 4000 rpm and 4 ℃ for 10 min before the supernatant was passed through a 0.22 μm filter and stored at −20 ℃. To evaluate auto-induction from the hydroxycinnamic acid inducible pC1622-PadR-CE1-GFP expression cassette, BS01-*CE1-GFP* or BS01-*GFP* were grown overnight in LB at 37 ℃ and used to inoculate 1 mL EZ Rich Defined Medium (Teknova) + Kan_{50} with either 1 mM ferulic acid or 6-*O*-feruloyl-D-glucose. All experiments were performed in a BioLector microfermentation system in 48-well Flowerplates® (m2p-labs) at 37 ℃. Bacterial growth was monitored via backward scattered light measurement at 620 nm, and GFP expression levels were monitored at an excitation of 488 nm and emission of 520 nm. The signal is given in arbitrary units [A.U.].

To evaluate *in situ* hydroxycinnamic acid release from corncob by strain BS01-*XynZ*, first a cellulolytic hydrolysis of 12.5 % (w/w) corncob was performed using 15 mg CTEC-2/g corncob in 150 mM citrate–phosphate buffer pH 5.0 at 50 ℃ for 48 h. The slurry was then neutralized to a pH of 7.0 and M9 salts and trace elements were added (6.78 g/L Na_2HPO_4, 3 g/L KH_2PO_4, 0.5 g/L NaCl, 1 g/L NH_4Cl, 2 mM $MgSO_4$, 100 μM $CaCl_2$, 1x trace elements) + Kan_{50}. The neutralized corncob slurry was inoculated with a relevant strain of *B. subtilis* to an OD_{600} of 0.1 and incubated at 37 ℃ and 180 rpm with intermittent sampling to determine OD_{600}, hydroxycinnamic acid release.

2.5. E. coli cultivation

Precultures of *E. coli* BL21(DE3) harbouring pET28a expression plasmid (see Supplementary Materials) grown overnight in LB at 37 ℃ were used to inoculate 10 mL of LB + Kan_{50} to an OD_{600} of 0.05, in triplicate. Cultures were incubated at 37 ℃ and 180 rpm. When an OD_{600} of 1 was reached, cultures were induced with 50 μM IPTG and incubated for a further 2 h before the addition of 2.5 mM of either coniferol or coumarol, and a 20 % (v/v) trimethyl pentane (TMP) top layer (with the exception of those cultures producing coniferyl methyl ether). After 18 h, the OD_{600} was measured, and both the aqueous phase and organic top layer were harvested for quantification of substrate conversion using HPLC and GC–MS.

Precultures of *E. coli* BL21(DE3) harbouring pROB expression cassettes were grown overnight in LB at 37 ℃ and used to inoculate 10 mL of M9 + Kan_{50} and 20 g/L glucose to an OD_{600} of 0.05, in triplicate. When an OD_{600} of 1 was reached, 2.5 mM of either ferulic or coumaric acid and a 20 % (v/v) trimethyl pentane (TMP) top layer was added. After 24 h, cultures were analysed as described above.

2.6. Co-culture

Cellulolytic hydrolysis of 12.5 % (w/v) corncob slurry was carried out as described above with intermittent sampling to quantify glucose/xylose release. Neutralized slurry + M9 salts and trace elements + Kan_{50} was inoculated to a final OD_{600} of 0.1 with a 1:1, 1:2 or 2:1 ratio of *B. subtilis* BS01-*XynZ-GFP* and EC-*CAAT-mCh* (individually pre-cultured in M9 with 0.5 % glucose + 0.5 % (w/v) xylose) and incubated at 37 ℃ and 180 rpm. A 20 % (v/v) TMP organic phases was added 10 h after inoculation. Co-cultures were incubated for 48 h with intermittent sampling to determine OD_{600}, GFP and mCherry fluorescence, glucose/xylose consumption and hydroxycinnamic acid/alcohol accumulation in the aqueous phase, and product accumulation in the organic phase.

2.7. Analytics

2.7.1. Quantification of glucose and xylose by HPLC

10 μL of neat 0.22 μm filtered culture supernatant or assay hydrolysate was injected onto and separated by a Supelcogel™ C–610H (6 % Crosslinked) column operating at 30 ℃ with an isocratic 0.1 % (v/v) H_3PO_4 mobile phase run at a flow rate of 0.5 mL/min. Sugars were quantified in the RID, with product identification and quantification carried out using authentic standards.

2.7.2. Quantification of ferulic acid, coumaric acid, Coniferol, coumarol and coniferyl methyl ether by HPLC

400 μL of 0.22 μm filtered culture supernatant or enzyme hydrolysate were appropriately diluted and combined with 400 μL methanol prior to injection of 5 μL onto an Avantor® ACE 5 C18-AR column operating at 30 ℃. A mobile phase of water (A) and acetonitrile (B) at a constant flow rate of 1 mL/min was run using the following gradient: 80 % A to 20 % A from 0 to 6 min, 20 % A to 80 % A from 6 to 7 min, and 80 % A from 7 to 11 min. Compounds were analysed in the UV at 254 nM. Product identification and quantification was carried out using authentic standards.

2.7.3. Quantification of acetate esters, Eugenol, Isoeugenol, chavicol by GC–MS

Volatile products were quantified using an Agilent Technologies 5975 MSD coupled to a 7890B GC with a PAL RSI 85 autosampler and an Agilent VT-5HP column (30 m × 0.25 mM × 0.1 μM). Injector temperature was set to 240 ℃ with a split ratio of 1:100 (1 μL injection). Column temperature was held at 140 ℃ for 5 min before ramping at 10 ℃/min to 300 ℃ and being held for 7 min. Ion source temperature of the mass spectrometer (MS) was set to 230 ℃ and spectra was recorded from *m/z* 50 to *m/z* 550. Compound identification was carried out using authentic standards and comparison to the reference spectra in the NIST library.

3. Results and discussion

3.1. Development of a B. subtilis hydroxycinnamic acid hydrolysis module

In order to achieve *in situ* release of ferulic and coumaric acid from the lignocellulose matrix in the extracellular environment, a hydrolytic enzyme module was installed in a suitable secretion strain. The robust and well characterised gram-positive bacterium *B. subtilis* was selected as the chassis strain for this module as, natively, it has a high capacity to secrete proteins (Harwood and Cranenburgh, 2008). To optimise this module within B. subtilis the following tasks were undertaken: (i) optimisation of protein secretion efficiency/extracellular protein preservation, (ii) elimination of endogenous metabolism that competes for ferulic and coumaric acid, and (iii) development a self-regulating protein secretion system. Natively, hydroxycinnamic acids are toxic to gram-positive bacteria such as *B. subtilis* and induce the phenolic acid stress response (PASR) which converts the phenolic acid to their non-toxic vinyl derivate via the phenolic acid decarboxylase, PadC (Tran et al., 2008). It was found that wild-type *B. subtilis* 168 was able to convert 5 mM of ferulic and coumaric acid to vinyl guiacol and vinyl phenol, respectively, via PadC within 4 h of initial exposure (Fig. 1A). To eliminate the activity of PadC, a simultaneous knockout/knock-in was performed whereby a constitutively expressed operon harbouring *prsA* and a partial *dnaK* operon were inserted into the genome at the site of *padC*. PrsA is an extracellular foldase that supports post-translocational folding of secreted protein, while the DnaK series are intracellular chaperones which maintain pre-proteins in translocation-competent conformation and minimizes aggregation. Over-expression of both has been previously shown to improve heterologous protein secretion between 9 and 12 fold in *B. subtilis* (Geissler et al., 2022; Chen et al., 2015). This genetic knockout/knock-in was performed in *B. subtilis* KO7, a strain deficient in seven extracellular proteases (Δ*nprE*, Δ*aprE*, Δ*erp*, Δ*mpr*, Δ*nrpB*, Δ*vrp*, Δ*bpr*), in order to promote retention of secreted target proteins in the extracellular environment. The resulting strain, BS01, had significantly reduced ability to convert exogenously supplied ferulic and coumaric acid to their vinyl derivatives (Fig. 1A). Unexpectedly, it was found that prolonged incubation of strain BS01 with ferulic and coumaric acid still resulted in some aromatic loss, 17 % and 25 % respectively upon extended incubation (see Supplementary Materials). As both of these compounds have low volatility, their loss is likely due to the activity of promiscuous endogenous *B. subtilis* enzymes.

Next, the development of a dynamic self-regulated expression system for those hydrolytic enzymes that will be targeted for secretion was pursued, such that their transcription is only activated in the presence of an effector derived from the lignocellulose. Such a biosensor-actuator system should avoid the metabolic burden associated with constitutive expression and the additional financial costs associated with the use of an exogenous inducer. To achieve this, *B. subtilis'* native *padC* regulatory machinery was exploited whereby the transcriptional repressor PadR represses *padC* expression by binding the P_{PadC} promoter. This repression is alleviated by the presence of ferulic, coumaric and caffeic acid which bind PadR and cause a conformational change that releases it from P_{PadC} (Nguyen et al., 2011; Tran et al., 2008). To test the functionality of this regulation as a hydroxycinnamic inducible biosensor, a biosensor reporter plasmid was constructed with the *padR* gene under the control of the constitutive P_{xylR} promoter and sf*GFP* under the control of $P_{Veg\text{-}PadO}$, a chimeric promoter consisting of the strong constitutive P_{Veg} promoter and the operator site of the P_{PadC} promoter (see Supplementary Materials). Both ferulic and coumaric acid were confirmed as having the ability to induce GFP expression from the biosensor, with a dynamic range of 64.6 and 56.1-fold respectively (Fig. 1B). Next, the ability of this biosensor to induce its own expression in the presence of a hydroxycinnamate ester was assessed, as would be

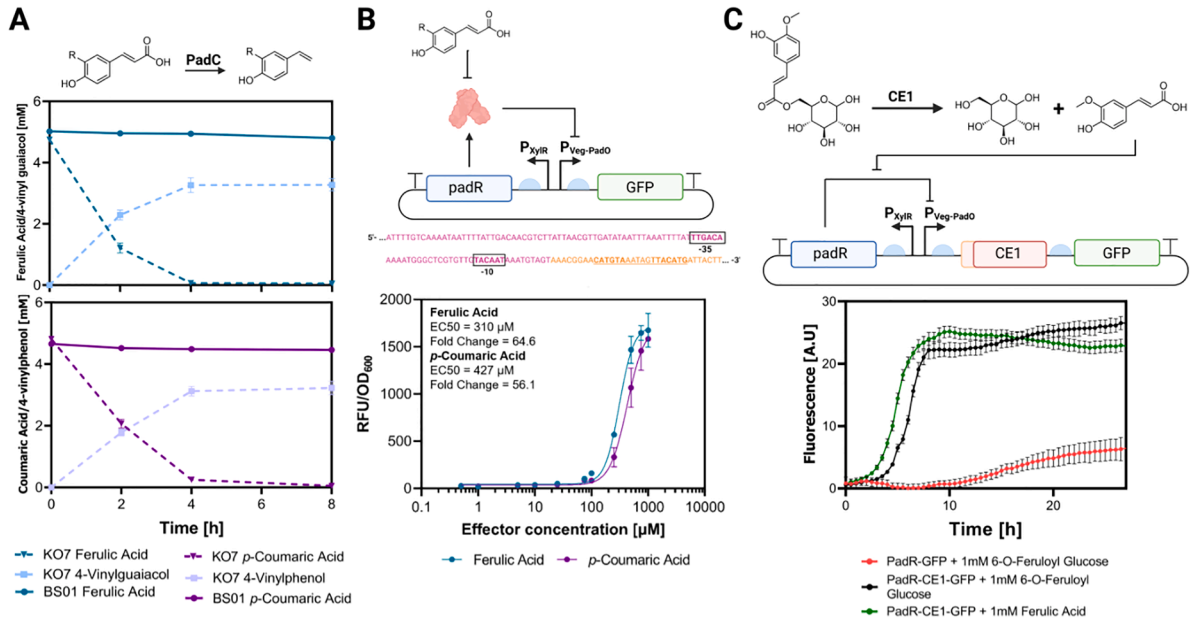

Fig. 1. Engineering of *B. subtilis* metabolism and development of hydroxycinnamic acid inducible biosensor. **A.** Comparison of the ability of *B. subtilis* BS01 and KO7 to degrade ferulic and coumaric acid to their vinyl derivatives via unperturbed (KO7) or perturbed (BS01) PadC activity. **B.** Above shows a schematic of the hydroxycinnamic acid responsive biosensor with the sequence of P_{Veg} promoter (purple) and the P_{PadO} (orange) operator site. The −35 and −10 sites of P_{veg} are boxed and the 18 bp region of the operator site that PadR binds is underlined. Within this region, the palindromic repeats of 6 bp are in bold. Below shows the dose response curves of the hydroxycinnamic acid biosensor to both ferulic and coumaric acid in BS01. **C.** Above shows a schematic of the hydroxycinnamic acid inducible cassette containing the ferulic acid esterase CE1 with its native signal peptide and its proposed method of auto-induction in the presence of a ferulic acid ester substrate. Below shows the accumulation of GFP by BS01-*GFP* in the presence of 6-*O*-feruloyl glucose or BS01-*CE1-GFP* in the presence of either ferulic acid (FA) or 6-*O*-feruloyl glucose. All data points are mean ± standard deviation of n = 3 biological replicates. R = H (*p*-coumaric acid/4-vinyl phenol) R = OMe (ferulic acid/4-vinyl guiacol).

the case with a lignocellulosic substrate. To do this, the signal peptide and feruloyl esterase domain (*CE1*) of *XynZ*, from *Clostridia thermocellum*, were inserted into the biosensor cassette upstream of sf*GFP*, to afford a combined biosensor-actuator/reporter. Cultures of BS01 harbouring this biosensor-actuator plasmid, named BS01-*CE1-GFP*, were exogenously supplemented with 6-*O*-feruloyl glucose as an example of a non-membrane permeable esterified ferulic acid substrate. As such, 6-*O*-feruloyl glucose hydrolysis should occur only in the extracellular environment as a result of secreted CE1 activity. sfGFP expression was monitored over 32 h and compared to cultures of BS01 harbouring the biosensor-reporter cassette without CE1, named BS01-*GFP*, in the presence of 6-*O*-feruloyl glucose and cultures of BS01-*CE1-GFP* in the presence of ferulic acid (Fig. 1C). In the absence of CE1, no significant GFP expression was observed as the extracellular esterase activity was insufficient to hydrolyse 6-*O*-feruloyl glucose and the ester was presumably unable to permeate into the cytoplasm. In the presence of CE1, basal expression and secretion from the cassette was sufficient for extracellular hydrolysis of 6-*O*-feruloyl glucose and subsequent induction of GFP (and CE1) by the released ferulic acid following, creating a positive feedback loop (Fig. 1C). Despite a 2-hour delay in the onset of induction, this system behaved similarly to the positive control where BS01-*CE1-GFP* was grown in the presence of free ferulic acid. On a more complex substrate, such as lignocellulose, the observed basal expression/secretion would afford sufficient activity to release an initial amount of ferulic and/or coumaric acid, and auto-induction of this cassette.

3.2. *In vitro* enzyme selection for high level release of hydroxycinnamic acids from lignocellulose

Ferulic and coumaric acid crosslink the hemicellulose and lignin fractions in plant cell wall. They are also ester-linked via their carboxylic acid group to the C(O)5 position of arabinofuranosyl side group of the xylan polymer of hemicellulose and ether-linked via the hydroxyl on their aromatic ring to the benzyl position or β-position of lignin. They can also be dimerised at the 5,5′- or 5,8′- positions (Wang et al., 2022; Lam et al., 2001). While feruloyl esterases (EC.3.1.1.73) are able to efficiently hydrolyse the ester bond linking these aromatic residues to polysaccharides within the hemicellulose fraction, it is unclear what enzymes are responsible for releasing ether-linked FA and CA associated with the lignin fraction. In nature lignocellulose degrading enzymes work synergistically to deconstruct the polymer, therefore to explore the impact of both direct acting and auxiliary acting enzymes on the efficiency of FA and CA release from lignocellulose a combinatorial comparison of FA/CA release *in vitro* from milled corncob by a ferulic acid esterase (CE1) alone, and in combination with lignolytic and hemicelluloytic enzymes. The lignolytic enzymes included were the multicopper oxidases CueO from *Ochrobactrum* sp. (Granja-Travez et al., 2018) and CopA from *Pseudomonas putida* (Granja-Travez and Bugg, 2018), and the Dyp-type peroxidase Dyp1B from *Pseudomonas fluorescens* (Rahmanpour and Bugg, 2015), while hemicellulolytic enzymes were the *endo*-1,4-β-xylanase (Xyl) from a rumen microorganism, an α-L-arabinofuranosidase (AraF) from *A. niger*, and an α-glucuronidase (α-gluc) from *C. japonicus*. FA/CA release was assessed after a 24 incubation of 10 % (w/v) milled corncob with purified enzyme *in vitro* (Fig. 2A). Treatment with CE1 alone yielded 170.5 ± 14.2 mg/L of combined FA and CA, while the addition of lignin acting CueO, CopA, and Dyp1B showed no improvement on the release of ferulic and coumaric acid compared the CE1 treatment alone, suggesting they are not releasing FA/CA from their ether-bonds. It should be noted, however, that evaluating lignin oxidising enzymes *in vitro* is made difficult by the generation of phenoxy radicals that can spontaneously repolymerise the substrate (Rashid and Bugg, 2021).

Of the hemicellulose acting enzymes, the arabinofuranosidase treatment resulted in no significant improvement in FA/CA release, while the α-glucuronidase and xylanase resulted in a 117 % and 170 %

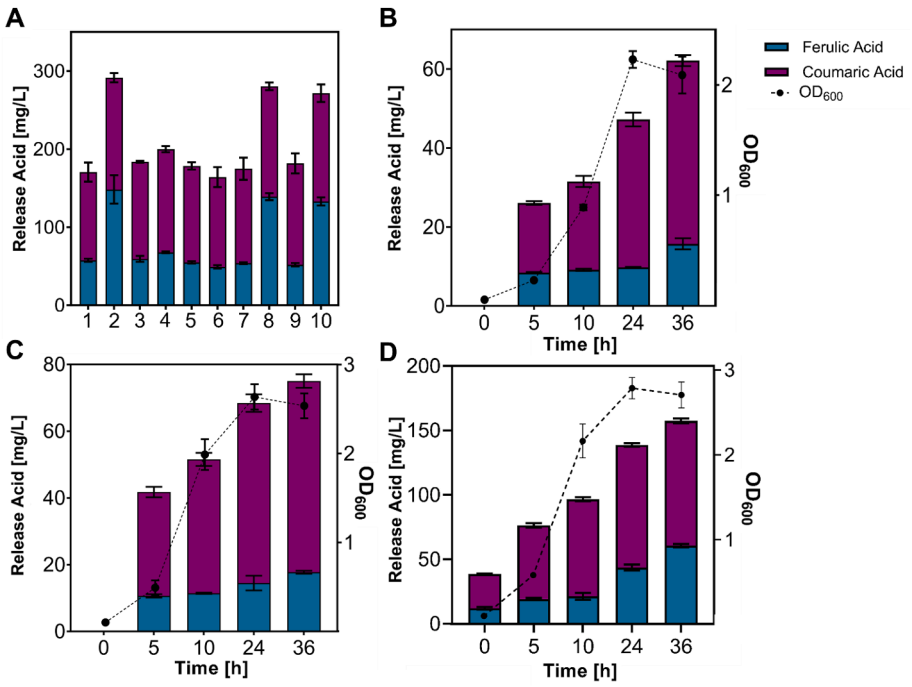

Fig. 2. Optimization of hydroxycinnamic acid release by an engineered *B. subtilis* secretion module. **A.** Comparison of the *in vitro* release of ferulic and coumaric acid from 10 % (w/v) corncob by CE1 alone or CE1 in combination with the hemicellulases or lignin oxidising enzymes. 1, CE1; 2, CE1 + Xyl; 3, CE1 + AraF; 4, CE1 + α-Gluc; 5, CE1 + Dyp1B; 6, CE1 + CopA; 7, CE1 + CueO; 8, CE1 + Xyl + AraF + α-Gluc; 9, CE1 + Dyp1B + CopA + CueO; 10, CE1 + Xyl + AraF + α-Gluc + Dyp1B + CopA + CueO. **B-D.** *In vivo* release of ferulic and coumaric acid over time by BS01 from 12.5 % (w/v) virgin corncob (B), BS01-*XynZ* from 12.5 % (w/v) virgin corncob (C), and BS01-*XynZ* from 12.5 % (w/v) pre-saccharified corncob (D). Culture OD_{600} is represented by the dashed line. All data points are mean ± standard deviation of n = 3 biological replicates.

improvement, respectively (Fig. 2A). However, those condition in which α-gluc and Xyl were combined did not result in a further improvement in FA/CA release over Xyl treatment alone. Interestingly, all trialled conditions that included xylanase activity demonstrated improved ferulic acid release, increasing its proportion to 50 % of the total aromatics released (compared to ~ 30 % in the absence of the xylanase). This would suggest that a greater proportion of ferulic acid is buried within the hemicellulose fraction, requiring cleavage of the xylan chain by the *endo*-1,4-β-xylanse activity to disrupt the hemicellulose structure and make the ester-linked FA more accessible to CE1. This is in agreement with previously studies where synergistic cooperation between a ferulic acid esterase and xylanases to release FA from wheat bran and corncob has been demonstrated (Lau et al., 2020).

The CE1 and xylanase treatment here resulted in the release of a combined total of 2.9 ± 0.2 g/Kg corncob of ferulic acid coumaric acid, which is 40 % of the total reported content of these acids in this feedstock, as determined by alkaline hydrolysis (Lau et al., 2019). To further improve upon this release, the impact of a pre-saccharification step (with the cellulolytic enzyme cocktail CTec-2) upon the subsequent release of ferulic and coumaric acid by CE1 + Xyl was evaluated, hypothesising that the additional polymer degradation would further aide in making the aromatic residues within lignocellulosic matrix more accessible. Here it was found that while cellulase pre-treatment alone resulted in only a small amount of FA and CA release (223.8 ± 8.5 mg/Kg), it had a significant impact on the FA/CA titres achieved via the subsequent CE1 + Xyl treatment, improving the combined yield to 3.7 ± 0.06 g/Kg corncob (see Supplementary Materials).

3.3. *In vivo release of hydroxycinnamic acids from corncob by a B. subtilis hydrolysis module*

As the combination of CE1 and a xylanase activity resulted the in highest yield of ferulic and coumaric acid release from milled corncob when exogenously supplied, the entire *XynZ* gene from *C. thermocellum* was selected for expression from the hydroxycinnamic acid inducible secretion cassette designed for *B. subtilis*. XynZ contains an N-terminal signal peptide/CE1 domain and C-terminal xylanase domain (Blum et al., 2000). The resulting strain was named BS01-*XynZ*. The ability of this strain to secrete XynZ and release FA and CA from a lignocellulose substrate *in vivo* was evaluated on both virgin corncob (no enzymatic pre-treatment) and saccharified corncob (pre-treated with CTec-2). BS01-*XynZ* grown in the presence of saccharified corncob solely utilised the sugars released from the pre-saccharification step for growth, while BS01-*XynZ* cultures grown in the presence of virgin corncob were supplemented with 10 g/L glucose.

The *in vivo* hydrolysis time courses demonstrated that BS01-*XynZ* can successfully release ferulic and coumaric acid from both corncob substrates, with cultures grown in the presence of the virgin corncob releasing a combined FA/CA titre of 76.1 ± 2.4 mg/L (0.61 ± 0.02 g/Kg), and cultures grown in the presence of the saccharified corncob releasing 159.6 ± 3.1 mg/L (1.28 ± 0.02 g/Kg; Fig. 2C&D). The significant improvement in aromatic release on the saccharified substrate is likely due to the pre-saccharification likely decreasing the recalcitrance of the lignocellulose matrix, making it more accessible to the activity of secreted XynZ during the *in vivo* hydrolysis. As well, the minor presence of both ferulic and coumaric acid in the initial medium (12 ± 1 mg/L and 26 ± 0.2 mg/L, respectively), which was released during the pre-saccharification step. Being so, expression and secretion of XynZ from the hydroxycinnamic acid inducible biosensor-actuator likely occurred earlier in this condition compared to the virgin corncob condition where there was no detectible ferulic or coumaric acid in the initial medium (Fig. 2C). This is consistent with the results of *BS01-GFP* grown in the presence of free or esterified FA, where expression of GFP occurred earlier in the former condition (Fig. 1C).

It was found that the parental strain BS01, without the XynZ secretion module, was also able to release ferulic and coumaric acid from both virgin and saccharified corncob, 61.1 ± 2.8 mg/L and 92.7 ± 7.4 m/L respectively (Fig. 2B, see Supplementary Materials). This suggests

that a portion of the ferulic and coumaric acid released from the lignocellulose substrate during cultivation with BS01-*XynZ* is a result of endogenous secreted esterase and/or lipase activity (Eggert et al., 2003). Despite this, targeted XynZ secretion by *B. subtilis* resulted in a significant improvement of hydroxycinnamic acid release from corncob compared to BS01, with 122 % and 166 % improvement in FA/CA titre when grown in the presence of virgin and saccharified corncob, respectively. The *B. subtilis* auto-induction secretion system demonstrated here has the potential to be expanded towards other lignocellulose hydrolysis enzymes in order to introduce novel functionality or overcoming endogenous regulation without the need for exogenous induction or the burden of continuous expression/protein secretion.

3.4. Development of an E. coli biotransformation module

Previously, Tramontina et al., (2020) demonstrated the efficient conversion of ferulic and coumaric acid to their monolignol alcohol derivatives, coniferol and coumarol, in *E. coli* via the expression of a carboxylic acid reductase (CAR5) from *Nocardia iowensis* and an aldo–keto reductase (AKR) from *Coptotermes gestroi*. *In planta,* these alcohols are precursors for the synthesis of volatile phenylpropenes and esters which play a role in plant communication, and which are widely applied to the perfume, flavour and pharmaceutical industries (Dhar et al., 2020). By heterologously reconstituting these biosynthetic pathways in *E. coli* biotransformation modules for the targeted conversion of lignocellulose released ferulic and coumaric acid to commercially relevant end-products can be developed. Assigning biotransformation modules to one host of a co-culture CBP permits a high degree of plug-and-play flexibility, which is increasingly relevant as biorefinery platforms continue to gain territory from their petrochemical counterparts and expand their spectrum of marketable biochemicals. Due the previously established biotransformation modules (Tramontina et al., 2020), here E. coli was selected as the production module host strain. However, in principle this module could also be established in other suitable microbial production hosts.

Further to coniferol and coumarol themselves, several commercially valuable derivatives include: (i) their acetate esters, which have application in the flavour and fragrance industry (Tramontina et al., 2023) and could be produced via the activity of an alcohol acyl transferase (AAT), (ii) their allyl/propenyl phenol derivatives which could be synthesised via an allyl/propenyl phenol synthase (IGS/EGS) from coniferyl or coumaryl acetate, and which, in addition to being fragrance and flavour additives, have use as antiseptics and in the formulation of resins and waterproofing membranes (Dhar et al., 2020; Dumas et al., 2016; Sung Su and Nam, 2010), and (iii) the 4-*O*-methyl ether of coniferol which could be achieved via a monolignol-4-*O*-methyl transferase (MOMT9), and which has been reported to have antiviral activity (Fig. 3A&F) (Tramontina et al., 2020).

To develop a suite of plug-and-play biotransformation pathways, a number of the chemical substrates and products for feasibility of production in a microbial co-culture were initially screened by assessing their microbial toxicity to both *E. coli* and *B. subtilis* (see Supplementary Materials). Several of these target end-products exhibited both high microbial toxicity and high volatility, which would necessitate *in situ* product recovery (ISPR) with an organic co-solvent to minimise both negative features. For this, several organic solvents of variable polarity were evaluated to identify a candidate capable of selectively extracting the volatile products and not the FA/CA substrates or their alcohol intermediates (instead leaving them in the aqueous phase), while also not hindering microbial growth (see Supplementary Materials). From these trials, the list of target end-products was narrowed to: coniferyl/coumaryl acetate, 4-*O*-coniferyl methyl ether, eugenol, isoeugenol, chavicol and isochavicol.

Several enzymes responsible for the required acetylation (AAT), allyl/propenyl phenol synthase (IGS/EGS), and methylation (MOMT9) biotransformations to achieve the desired end-products from ferulic or coumaric acid have been previously reported and validated as functional in microbial hosts (Dexter et al., 2007; Kim et al., 2014; Cai et al., 2015; Dhar et al., 2020). To identify the best enzyme candidate for each reaction step, biotransformation modules were developed by insertion of an AAT, IGS, EGS, or MOMT9 into a pET28 plasmid backbones and then used to transform *E. coli* BL21(DE3) (see Supplementary Materials). Feeding experiments were then performed whereby 2 mM of either intermediate alcohol, coniferol or coumarol, was exogenously supplemented into cultures of *E. coli* heterologously expressing a candidate enzyme, and then assessed for substrate conversion after 18 h (Fig. 3). Alcohol acyl transferases (AATs) from *E. coli* (CAT), *Larrea tridentata* (CAAT), *Petunia hybrida* (CFAT), *Ocimum bacilicum* (ObAAT), *Fragaria* × *ananassa* (SAAT), and *Clarkia breweri* (BEAT) were evaluated against both alcohols to identify the best acetylation candidate for each intermediate. Here it was found that all candidate AATs displayed activity towards coniferol, with CFAT, ObAAT, SAAT and BEAT producing similar titres of coniferyl acetate, while CAAT showed the lowest activity towards coniferol (Fig. 3B). Of the higher producers, CFAT expression resulted in 202.7 ± 2.8 mg/ L. The production of coniferyl diacetate by all the AATs was also observed, with the exception of CAAT (see Supplementary Materials). There was no detection of coniferyl monoacetate whereby the C4 hydroxyl group on the aromatic ring was acetylated, suggesting that the C9-OH is preferentially acetylated over the C4-OH (Fig. 3B). Conversely, only CAT, CAAT, and BEAT demonstrated activity towards coumarol, with all three converting it to coumaryl diacetate (no monoacetate was detected; Fig. 3G). The exclusive production of the diacetate suggests the second acylation reaction at C4-OH occurs more quickly for coumarol than for coniferol, presumably arising due to steric hinderance by the C3 methoxy group of coniferol.

E. coli expressing CAAT or BEAT additionally produced chavicol spontaneously, while chavicol acetate was also detected in the BEAT cultures (Fig. 3G; see Supplementary Materials), although it is unclear if chavicol acetate was derived from the acetylation of chavicol or the reduction of coumaryl acetate. Chavicol synthesis proceeds by the reductive cleavage of the C9 acetate moity of coumaryl acetate via an allylphenol synthase. Neither CAAT nor BEAT has been previously reported to possess this activity, suggesting that the reduction reaction is the result of promiscuous endogenous *E. coli* activity.

CFAT co-expressed with either an allylphenol synthase from *P. hybida* (PhEGS), *C. breweri* (CbEGS) or *O. basilicum* (ObEGS) to make eugenol, or the propenylphenol synthases PhIGS and CbIGS to make isoeugenol, from coniferol were all successful in producing their respective product (Fig. 3D&E). However, in all cases eugenol/isoeugenol titres were low with the majority of the accumulated product being the acetate and diacetate ester, suggesting the reduction reaction is rate limiting. This agrees with previous work where the concentrated cell lysate of an *E. coli* culture expressing CFAT and ObEGS produced 32.8 mg/L of eugenol from 3 mM of coniferol (Robinson et al., 2020). Lastly, an engineered monolignol-4-*O*-methyl transferase (MOMT9) from *C. breweri* with high selectively for coniferol was successfully employed to produce 194.8 ± 2.4 mg/L coniferyl methyl ether (Fig. 3C). Attempts to produce isochavicol from coumarol via co-expression of CAAT and a propenylphenol synthase from either *P. hybida* (PhIGS) or *C. breweri* (CbIGS) were unsuccessful (data not shown).

To demonstrate product formation directly from ferulic and coumaric acid, the genes encoding best candidate enzymes for the biosynthesis of coniferyl acetate, coniferyl diacetate, coumaryl diacetate, eugenol, isoeugenol, chavicol and chavicol acetate were assembled into a series of operons on a plasmid also containing the genes encoding CAR5, AKR and sfp variant (required to convert ferulic and coumaric acid to coniferol and coumarol, respectively) in a separate operon (Fig. 4A). Each *E. coli* biotransformation module (i-vii) was evaluated for its ability to convert 2.5 mM of exogenously supplied ferulic or coumaric acid to target end-product after a 24-hour incubation. Each module successfully turned over all exogenously supplied ferulic or coumaric acid to their respective alcohol intermediate and end-product after 24 h

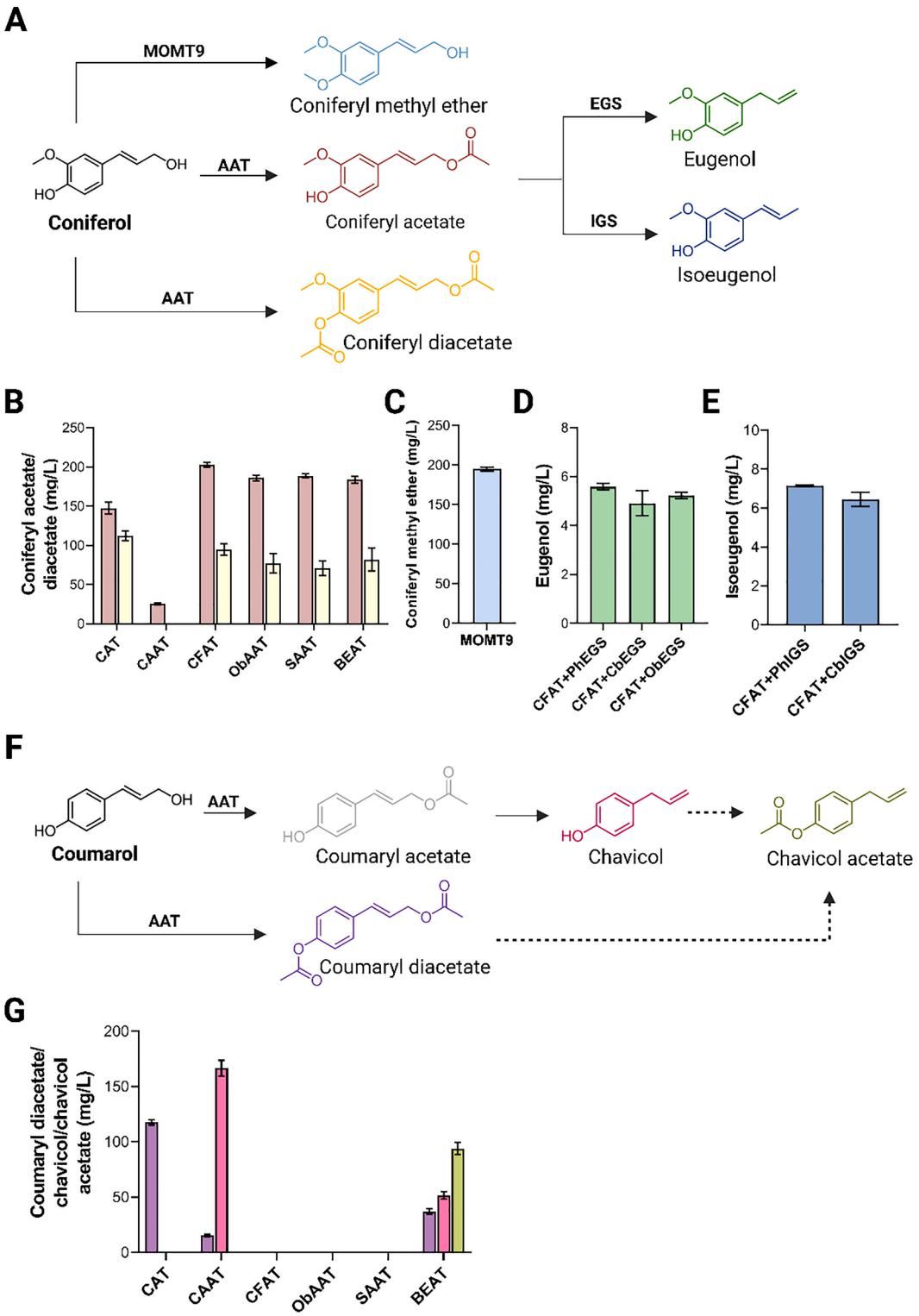

Fig. 3. Identification of the best enzyme candidates for each biotransformation step in *E. coli*. **A&F.** Illustration of the end products successfully produced by *E. coli* from exogenously supplied coniferol (A) and coumarol (F). formation with multiple potential routes shown with dashed arrows. **B-E & G.** *In vivo* product formation from 2 mM of exogenously supplied coniferol (B-E) and coumarol (G) by *E. coli* heterologously expressing CAT, CAAT, CFAT, ObAAT, SAAT, BEAT, PhEGS, CbEGS, ObEGS, PhIGS, CbIGS, or MOMT9. A 20 % (v/v) TMP organic extractive phase was used to capture coniferyl acetate (rose), coniferyl diacetate (yellow), eugenol (green), isoeugenol (dark blue), coumaryl diacetate (purple), chavicol (pink) and isochavicol (olive). Coniferol, coumarol and coniferyl methyl ether (light blue) were quantified from the aqueous phase. All data points are mean ± standard deviation of n = 3 biological replicates.

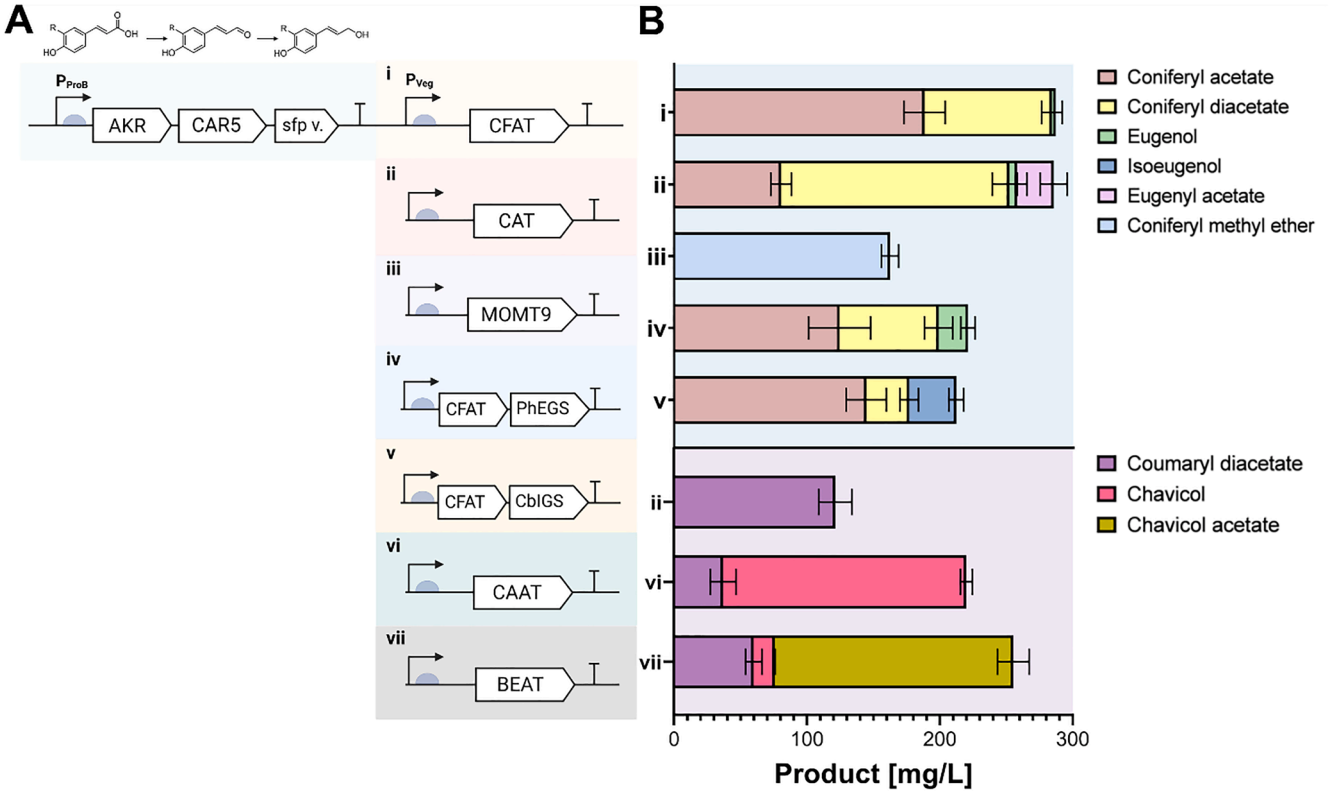

Fig. 4. Development of *E. coli* biotransformation modules for the conversion of ferulic and coumaric acid to value-added end products. **A**. Schematics to the left show modules i-vii composed of AKR, CAR5 and sfp variant to convert ferulic/coumaric acid to coniferol/coumarol, and the best candidate enzymes identified for each biotransformation step towards the target end product. **B**. product profiles achieved from 2.5 mM of ferulic or coumaric acid by *E. coli* heterologous expression of modules i-vii. All data points are mean ± standard deviation of n = 3 biological replicates.

(Fig. 4B, see Supplementary Materials). Each module's target end-product was the dominant species produced, with the exception of modules iv and v for eugenol and isoeugenol, respectively, where the IGS and EGS enzymes had already been shown to be rate limiting (Fig. 3B). Depending on the intended commercial application of the aromatic CBP, a product mixture may be desired (e.g., for flavour and fragrance use), however, should a singular end-product be the target, the *in situ* product removal (ISPR) strategy used here would significantly decrease the cost of product purification over traditional distillation. Additionally, protein engineering could also be used to further tailor product titres/ratios, with promising examples of such work recently having been demonstrated for the CAT enzyme (Seo et al., 2021).

3.5. Synthetic co-cultivation of engineered *B. subtilis* and *E. coli* for the consolidated hydrolysis and valorisation of corncob hydroxycinnamic acids

A critical criterion for the development of a successful synthetic consortium based bioprocess is a stable and tuneable population composition between the participating sub-strains, with stability affording consistency across batches and tunability permitting optimization for a desired output (Minty et al. 2013). To evaluate both the stability and tunability of *B. subtilis* and *E. coli* in a co-cultivation, a strain of BS01 constitutively expressing GFP (BS01-*conGFP*) and a strain of *E. coli* constitutively expressing mCherry (EC-*mCh*) were inoculated into discrete co-cultures at different initial ratios, and fluorescence was tracked to determine the proportion of each sub-population over time (see Supplementary Materials). Here it was found that the proportion of the populations at stationary phase were similar to the proportions in the initial inoculums, with neither species dominating over the other. The single exception to this was a co-culture inoculated at a ratio of 2:1 (BS01-*conGFP:EC-mCh)*, which at stationary phase was composed of 58 % EC-*mCh* (see Supplementary Materials). These results validate the compatibility of *B. subtilis* and *E. coli* as consortia partners, having demonstrated stable and tuneable co-growth.

To demonstrate value-added product formation directly from corncob lignocellulose, co-cultivation between the *B. subtilis* hydrolysis module and an *E. coli* biotransformation module was performed using BS01 expressing *XynZ* from the hydroxycinnamic acid inducible secretion cassette and a constitutively expressed GFP (named BS01-*XynZ-GFP*), and an *E. coli* expressing biosynthetic cassette vi modified to include a constitutively expressed *mCherry* (named EC-*CAAT-mCh*) for the production of chavicol. Fig. 5A illustrates the workflow for these cultivations, consisting of the (i) pre-saccharification of 12.5 % corncob (w/v), (ii) inoculation with BS01-*XynZ-GFP* and EC-*CAAT-mCh* and an organic phase for ISPR, and (iii) product recovery based on phase separation.

The pre-saccharification of corncob yielded approximately 12.5 g/L glucose and 3.3 g/L xylose (see Supplementary Materials). Three initial inoculation ratios of BS01-*XynZ-GFP*:EC-*CAAT-mCh* (BS:EC) were compared: 2:1, 1:1 and 1:2. The three co-cultures grew similarly (reaching a final OD_{600} of 3.09 ± 0.11, 2.94 ± 0.15 and 3.04 ± 0.23, respectively, after 48 h), and demonstrated similar glucose consumption rates (Fig. 5B). The co-culture inoculated with 2:1 ratio of BS:EC had a slower rate of xylose consumption, likely due to the fact that *B. subtilis* possesses poor xylose uptake (Schmiedel and Hillen, 1996). As such, *E. coli* is the primary consumer of xylose and the slower rate of consumption observed is likely a result of the lower proportion of this microbe within the co-culture. While both glucose and xylose were depleted by 36 h, growth continued for all co-cultures up to 48 h (Fig. 5B). Here, in addition to XynZ, *B. subtilis* will be secreting its endogenous β-xylanase (XynA) and β-xylosidase (XynB) and releasing

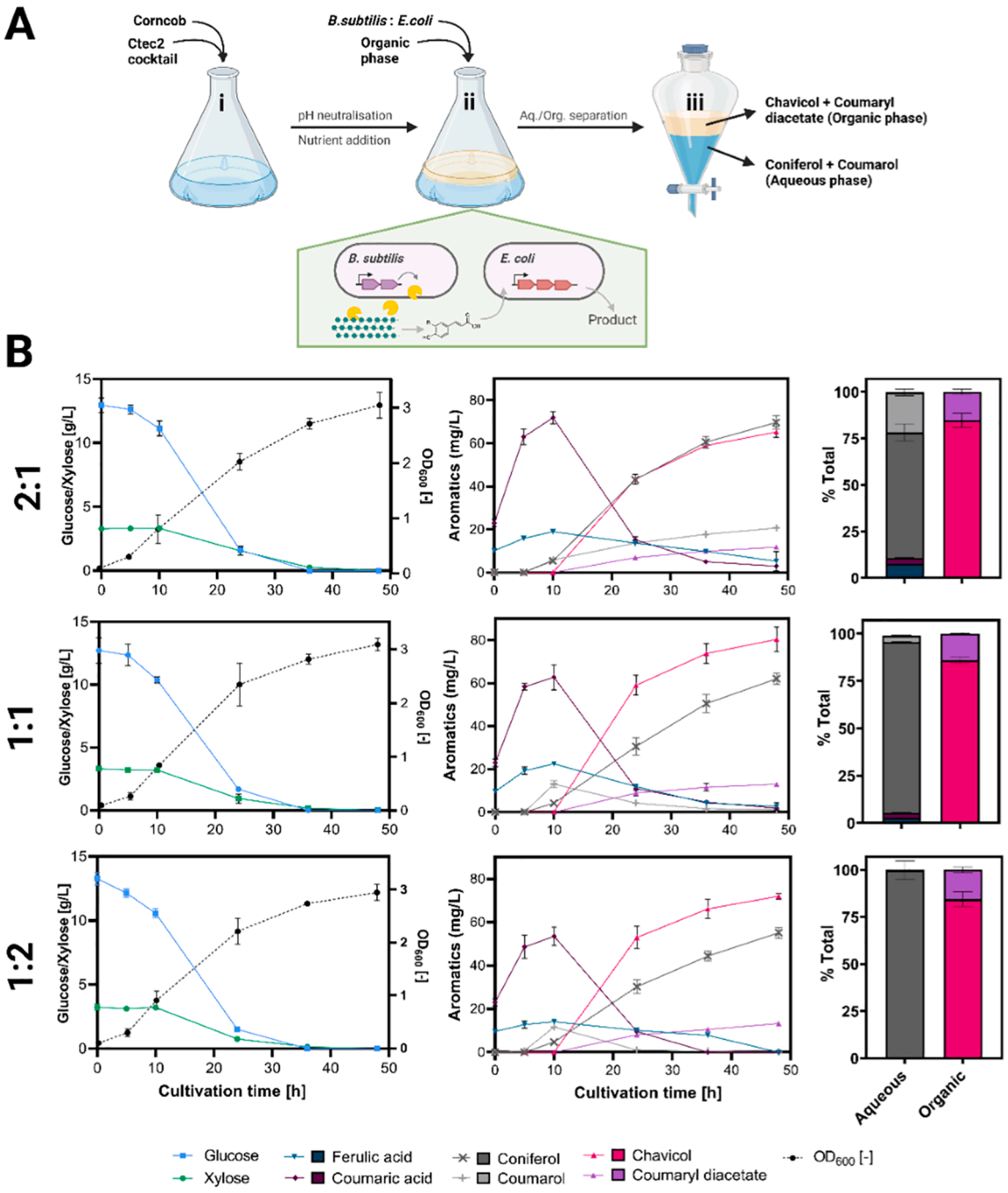

Fig. 5. Synthetic co-cultivation of BS01-*XynZ-GFP* and EC-*CAAT-mCh* for the consolidated release and conversion of corncob lignocellulose ferulic and coumaric acid to value products. **A.** Illustration of the co-cultivation workflow, consisting of: (i) an initial corncob saccharification step using 12.5 % (w/v) corncob and 15 mg C-Tec2/g corncob at pH 5.0 and 50 °C, followed by slurry neutralisation, (ii) co-inoculation of *B. subtilis* and *E. coli* for aromatic CBP at pH 7.0 and 37 °C in the presence of an organic phase, and a (iii) product isolation step based on phase separation. **B.** Utilisation of glucose and xylose for growth by *B. subtilis* and *E. coli* co-cultures at 2:1, 1:1, and 1:2 ratios (left), time courses of ferulic/coumaric acid release from lignocellulose and their biotransformation to end product (middle), and the proportion of each aromatic substrate, intermediate and product partitioned into the aqueous and organic phases after 48 h (right). All data points are mean ± standard deviation of n = 3 biological replicates.

xylose from the corncob substrate to supply a carbon source primarily for *E. coli* (Lindner et al., 1994). While unlike *E. coli*, *B. subtilis* is capable of assimilating the cellobiose released from corncob during the pre-saccharification and utilising it for growth via an intracellular phospho-β-glucosidase (LicH) (Parisutham et al., 2017).

Each co-culture maintained its initial inoculation ratio throughout the time course, as determined by GFP and mCherry (see Supplementary Materials). Despite not having been engineered for explicit co-dependency, co-cultivation was likely mutually beneficial for *B. subtilis* and *E. coli*, with *E. coli* benefitting from *B. subtilis*' cellulolytic activity and the *PadC* deficient BS01 benefiting from the quick removal of FA and CA from the environment via *E. coli* biotransformation. Such mutualistic interaction reinforces co-culture stability, which is essential for repeated batch fermentation or continuous culture.

All co-cultivations successfully resulted in the release of ferulic and coumaric acid from the corncob substrate via the activity of BS01-*XynZ-GFP*, and subsequent biotransformation of these acids via the activity of EC-*CAAT-mCh* (Fig. 5B). The appearance of coniferol and coumarol in

the medium began after 10 h, while the accumulation of chavicol and coumaryl diacetate began after 24 h. As CAAT selectively acted on coumarol and not coniferol, the latter polar alcohol accumulated in the aqueous phase while the less polar chavicol and coumaryl diacetate partitioned into the organic phase (Fig. 5B). The purposeful segregation of valuable end-products based on polarity could lower overall bioprocess costs as it permits multiple end-products to be synthesized in a single batch. Initial BS:EC inoculation ratio had an impact on total aromatic yield, with 173 ± 9.3 mg/L, 160 ± 11.3 mg/L, and 140.6 ± 7.0 mg/L achieved from the 2:1, 1:1 and 1:2 ratios, respectively, after 48 h (Fig. 5B). The highest product titre from the 2:1 ratio is likely a consequence of the higher proportion of *B. subtilis* in the co-culture, resulting in a larger release of FA and CA from the lignocellulose polymer. However, this ratio also resulted in the poorest FA/CA conversion, with residual FA, CA and coumarol present in the aqueous phase at 48 h as a consequence of the lower proportion of biotransformation activity by EC-*CAAT-mCh* module. The incomplete biotransformation of starting material/intermediates increases the heterogeneous mix of aqueous phase aromatics which is unfavourable for downstream products separation. The opposite trend is seen in the 1:2 co-culture, where overall there was lower end-product formation but high substrate conversion. Here, the aqueous phase was nearly exclusively composed of coniferol, representing 99.6 ± 4.9 % of the total. The intermediate inoculation ratio of 1:1 resulted in a middle ground for both product titre and substrate conversion compared to ratios 2:1 and 1:2 (Fig. 5B). These results highlight the importance of tuning the upstream and downstream modules of a co-cultivation in order to optimise product titre and purity.

Previous studies towards these target compounds have reported various production titres. For coniferol production via a consolidated process, using exogenously added hydrolytic enzymes and a wheat arabinoxylan feedstock, afforded 71 mg/L (Tramontina et al., 2020), whereas production via a de novo co-culture route, from glucose and glycerol, afforded 125 mg/L (Chen et al., 2017). For chavicol production via biotransformation of coumaric acid 28 mg/L was reported (Robinson et al., 2020), and via de novo co-culture route unquantified production was reported (Brooks et al., 2023). However, these studies have predominately used purified monosaccharides as a substrate for growth and bioproduction, or require additional processing steps for the production of the hydrolytic enzymes and biomass hydrolysis. In addition, the combined production-*in situ* separation demonstrated here avoids the need for purification costs, which can impact heavily upon the economic viability of any chemical/biochemical production process. Whilst full technoeconomic analysis is required to elucidate the impact of feedstock, capital, processing and purification costs, it is apparent the co-culture CBP is likely to be competitive against the previously reported multi-step production processes.

4. Conclusions

Using a synthetic co-culture platform consisting of an engineered *B. subtilis* hydroxycinnamic acid inducible hydrolysis module and an engineered *E. coli* biotransformation module, a targeted CBP strategy for the direct valorisation of lignocellulose incorporated ferulic and coumaric acid to coniferol and chavicol was demonstrated. It was found that a 1:2 BC:EC strain ratio was ideal for high product specificity and titre, with 55 ± 2.5 mg/L coniferol in the aqueous phase and 72 ± 1.3 mg/L chavicol in the organic phase. This study illustrates the potential of applying microbial consortia to the valorisation of individual lignocellulose associated aromatic monomers.

Declaration of Competing Interest

The authors declare that they have no known competing financial interests or personal relationships that could have appeared to influence the work reported in this paper.

Data availability

Data will be made available on request.

Acknowledgements

The authors would like the acknowledge Rehana Sung and the MIB separation facilities, Elizabeth Hardiman for the AT constructs, and Dr. David Tilly for synthesis of chemical standards.

Authors' contributions

MC and ND planned the experiments, MC performed the experiments, EP performed initial characterisation of SAAT and BEAT, TDHB provided the oxidase/laccase expression plasmids, MC and ND analysed the data and wrote the manuscript. All authors read and approved the final version of the manuscript.

Funding

This work was supported by the BBSRC responsive mode grant (BB/P01738X/1).

Appendix A. Supplementary data

Supplementary data to this article can be found online at https://doi.org/10.1016/j.biortech.2023.129935.

References

Alvarez-Gonzalez, G., Dixon, N., 2019. Genetically encoded biosensors for lignocellulose valorization. Biotechnol. Biofuels 12, 246. https://doi.org/10.1186/s13068-019-1585-6.

Barton, C., Horbal, L., Starck, S., Kohlstedt, M., Luzhetskyy, A., Wittmann, C., 2018. Enabling the valorization of guaiacol-based lignin Integrated chemical and biochemical production of cis, cis-muconic acid using metabolically engineered Amycolatopsis sp. ATCC 39116. Metab. Eng. 45, 200–210. https://doi.org/10.1016/j.ymben.2017.12.001.

Blum, D.L., Kataeva, I.A., Li, X.L., Ljungdahl, L.G., 2000. Feruloyl esterase activity of the *Clostridium thermocellum* cellulosome can be attributed to previously unknown domains of XynY and XynZ. J. Bacteriol. 182, 1346–1351. https://doi.org/10.1128/JB.182.5.1346-1351.2000.

Brooks, M.S., Marsan, C., Reed, K.B., Yuan, S.-F., Nguyen, D.-D., Trivedi, A., Altin-Yavuzarslan, G., Ballinger, N., Nelson, A., Alper, H., 2023. A tripartite microbial co-culture system for de novo biosynthesis of diverse plant phenylpropanoids. Nat. Commun. 14, 4448. https://doi.org/10.1038/s41467-023-40242-9.

Buanafina, M.M.O., 2009. Feruloylation in grasses: current and future perspectives. Mol. Plant. 2, 861–872. https://doi.org/10.1093/mp/ssp067.

Cai, Y., Bhuiya, M.W., Shanklin, J., Liu, C.J., 2015. Engineering a monolignol 4-O-methyltransferase with high selectivity for the Condensed Lignin Precursor Coniferyl Alcohol. J. Biol. Chem. 290, 26715–26724. https://doi.org/10.1074/jbc.M115.684217.

Chen, J., Fu, G., Gai, Y., Zheng, P., Zhang, D., Wen, J., 2015. Combinatorial Sec pathway analysis for improved heterologous protein secretion in *Bacillus subtilis*: Identification of bottlenecks by systematic gene overexpression. Microb. Cell Fact. 14, 1–15. https://doi.org/10.1186/s12934-015-0282-9.

Chen, Z., Sun, X., Li, Y., Yan, Y., Yuan, Q., 2017. Metabolic engineering of Escherichia coli for microbial synthesis of monolignols. Metab. Eng. 39, 102–109. https://doi.org/10.1016/j.ymben.2016.10.021.

Dexter, R., Qualley, A., Kish, C.M., Ma, C.J., Koeduka, T., Nagegowda, D.A., Dudareva, N., Pichersky, E., Clark, D., 2007. Characterization of a petunia acetyltransferase involved in the biosynthesis of the floral volatile isoeugenol. Plant J. 49, 265–275. https://doi.org/10.1111/j.1365-313X.2006.02954.x.

Dhar, N., Sarangapani, S., Reddy, V.A., Kumar, N., Panicker, D., Jin, J., Chua, N.H., Sarojam, R., 2020. Characterization of a sweet basil acyltransferase involved in eugenol biosynthesis. J. Exp. Bot. 71, 3638–3652. https://doi.org/10.1093/jxb/eraa142.

Dumas, L., Bonnaud, L., Olivier, M., Poorteman, M., Dubois, P., 2016. Chavicol benzoxazine: Ultrahigh Tg biobased thermoset with tunable extended network. Eur. Polym. J. 81, 337–346. https://doi.org/10.1016/j.eurpolymj.2016.06.018.

Eggert, T., Brockmeier, U., Dröge, M.J., Quax, W.J., Jaeger, K.E., 2003. Extracellular lipases from *Bacillus subtilis*: Regulation of gene expression and enzyme activity by amino acid supply and external pH. FEMS Microbiol. Lett. 225, 319–324. https://doi.org/10.1016/S0378-1097(03)00536-6.

Galman, J.L., Parmeggiani, F., Seibt, L., Birmingham, W.R., Turner, N.J., 2022. One-Pot Biocatalytic In Vivo Methylation-Hydroamination of Bioderived Lignin Monomers to

Generate a Key Precursor to L-DOPA. Angew. Chemie - Int. Ed. 61 https://doi.org/10.1002/anie.202112855.
Geissler, A.S., Poulsen, L.D., Doncheva, N.T., Anthon, C., Seemann, S.E., González-Tortuero, E., Breüner, A., Jensen, L.J., Hjort, C., Vinther, J., Gorodkin, J., 2022. The impact of PrsA over-expression on the *Bacillus subtilis* transcriptome during fed-batch fermentation of alpha-amylase production. Front. Microbiol. 13, 1–17. https://doi.org/10.3389/fmicb.2022.909493.
Granja-Travez, R.S., Bugg, T.D.H., 2018. Characterization of multicopper oxidase CopA from *Pseudomonas putida* KT2440 and *Pseudomonas fluorescens* Pf-5: Involvement in bacterial lignin oxidation. Arch. Biochem. Biophys. 660, 97–107. https://doi.org/10.1016/j.abb.2018.10.012.
Granja-Travez, R.S., Wilkinson, R.C., Persinoti, G.F., Squina, F.M., Fülöp, V., Bugg, T.D.H., 2018. Structural and functional characterisation of multi-copper oxidase CueO from lignin-degrading bacterium *Ochrobactrum* sp. reveal its activity towards lignin model compounds and lignosulfonate. FEBS J. 285, 1684–1700. https://doi.org/10.1111/febs.14437.
Hartline, C.J., Schmitz, A.C., Han, Y., Zhang, F., 2021. Dynamic control in metabolic engineering: Theories, tools and applications. Metab. Eng. 63, 126–140. https://doi.org/10.1016/j.ymben.2020.08.015.
Harwood, C.R., Cranenburgh, R., 2008. *Bacillus* protein secretion: an unfolding story. Trends Microbiol. 16, 73–79. https://doi.org/10.1016/j.tim.2007.12.001.
Kim, S.J., Vassão, D.G., Moinuddin, S.G.A., Bedgar, D.L., Davin, L.B., Lewis, N.G., 2014. Allyl/propenyl phenol synthases from the creosote bush and engineering production of specialty/commodity chemicals, eugenol/isoeugenol, in *Escherichia coli*. Arch. Biochem. Biophys. 541, 37–46. https://doi.org/10.1016/j.abb.2013.10.019.
Lam, T.B.T., Kadoya, K., Iiyama, K., 2001. Bonding of hydroxycinnamic acids to lignin: Ferulic and p-coumaric acids are predominantly linked at the benzyl position of lignin, not the β-position, in grass cell walls. Phytochemistry 57, 987–992. https://doi.org/10.1016/S0031-9422(01)00052-8.
Lau, T., Harbourne, N., Oruña-Concha, M.J., 2019. Valorisation of sweet corn (Zea mays) cob by extraction of valuable compounds. Int. J. Food Sci. Technol. 54, 1240–1246. https://doi.org/10.1111/ijfs.14092.
Lau, T., Harbourne, N., Oruña-Concha, M.J., 2020. Optimization of enzyme-assisted extraction of ferulic acid from sweet corn cob by response surface methodology. J. Sci. Food Agric. 100, 1479–1485. https://doi.org/10.1002/jsfa.10155.
Lindner, C., Stulke, J., Hecker, M., 1994. Regulation of xylanolytic enzymes in *Bacillus subtilis*. Microbiology 140, 753–757. https://doi.org/10.1099/00221287-140-4-753.
Linger, J.G., Vardon, D.R., Guarnieri, M.T., Karp, E.M., Hunsinger, G.B., Franden, M.A., Johnson, C.W., Chupka, G., Strathmann, T.J., Pienkos, P.T., Beckham, G.T., 2014. Lignin valorization through integrated biological funneling and chemical catalysis. PNAS 111. https://doi.org/10.1073/pnas.1410657111.
Liu, L., Yang, J., Yang, Y., Luo, L., Wang, R., Zhang, Y., Yuan, H., 2019. Consolidated bioprocessing performance of bacterial consortium EMSD5 on hemicellulose for isopropanol production. Bioresour. Technol. 292, 121965 https://doi.org/10.1016/j.biortech.2019.121965.
Mazzoli, R., 2021. Current progress in production of building-block organic acids by consolidated bioprocessing of lignocellulose. Fermentation 7. https://doi.org/10.3390/fermentation7040248.
Minty, J.J., Singer, M.E., Scholz, S.A., Bae, C.H., Ahn, J.H., Foster, C.E., Liao, J.C., Lin, X.N., 2013. Design and characterization of synthetic fungal-bacterial consortia for direct production of isobutanol from cellulosic biomass. PNAS 110, 14592–14597. https://doi.org/10.1073/pnas.1218447110.
Nguyen, T.K.C., Tran, N.P., Cavin, J.F., 2011. Genetic and biochemical analysis of PadR-padC promoter interactions during the phenolic acid stress response in *Bacillus subtilis* 168. J. Bacteriol. 193, 4180–4191. https://doi.org/10.1128/JB.00385-11.
Parisutham, V., Chandran, S.P., Mukhopadhyay, A., Lee, S.K., Keasling, J.D., 2017. Intracellular cellobiose metabolism and its applications in lignocellulose-based biorefineries. Bioresour. Technol. 239, 496–506. https://doi.org/10.1016/j.biortech.2017.05.001.
Rahmanpour, R., Bugg, T.D.H., 2015. Characterisation of Dyp-type peroxidases from Pseudomonas fluorescens Pf-5: Oxidation of Mn(II) and polymeric lignin by Dyp1B. Arch. Biochem. Biophys. 574, 93–98. https://doi.org/10.1016/j.abb.2014.12.022.
Rashid, G.M.M., Bugg, T.D.H., 2021. Enhanced biocatalytic degradation of lignin using combinations of lignin-degrading enzymes and accessory enzymes. Cat. Sci. Technol. 11, 3568–3577. https://doi.org/10.1039/d1cy00431j.
Rinaldi, R., Jastrzebski, R., Clough, M.T., Ralph, J., Kennema, M., Bruijnincx, P.C.A., Weckhuysen, B.M., 2016. Paving the Way for Lignin Valorisation: Recent Advances in Bioengineering, Biorefining and Catalysis. Angew. Chemie - Int. Ed. 55, 8164–8215. https://doi.org/10.1002/anie.201510351.
Robinson, C.J., Carbonell, P., Jervis, A.J., Yan, C., Hollywood, K.A., Dunstan, M.S., Currin, A., Swainston, N., Spiess, R., Taylor, S., Mulherin, P., Parker, S., Rowe, W., Matthews, N.E., Malone, K.J., Le Feuvre, R., Shapira, P., Barran, P., Turner, N.J., Micklefield, J., Breitling, R., Takano, E., Scrutton, N.S., 2020. Rapid prototyping of microbial production strains for the biomanufacture of potential materials monomers. Metab. Eng. 60, 168–182. https://doi.org/10.1016/j.ymben.2020.04.008.
Salvachúa, D., Karp, E.M., Nimlos, C.T., Vardon, D.R., Beckham, G.T., 2015. Towards lignin consolidated bioprocessing: simultaneous lignin depolymerization and product generation by bacteria. Green Chem. 17, 4951–4967. https://doi.org/10.1039/c5gc01165e.
Schmiedel, D., Hillen, W., 1996. A *Bacillus subtilis* 168 mutant with increased xylose uptake can utilize xylose as sole carbon source. FEMS Microbiol. Lett. 135, 175–178. https://doi.org/10.1016/0378-1097(95)00445-9.
Schmitz, E., Leontakianakou, S., Norlander, S., Nordberg Karlsson, E., Adlercreutz, P., 2022. Lignocellulose degradation for the bioeconomy: The potential of enzyme synergies between xylanases, ferulic acid esterase and laccase for the production of arabinoxylo-oligosaccharides. Bioresour. Technol. 343, 126114 https://doi.org/10.1016/j.biortech.2021.126114.
Seo, H., Lee, J.-H., Giannone, R.J., Dunlap, N.J., Trinh, C.T., 2021. Engineering promiscuity of chloramphenicol acetyltransferase for microbial designer ester biosynthesis. Metab. Eng. 66, 179–190. https://doi.org/10.1016/j.ymben.2021.04.005.
Sethupathy, S., Murillo Morales, G., Gao, L., Wang, H., Yang, B., Jiang, J., Sun, J., Zhu, D., 2022. Lignin valorization: Status, challenges and opportunities. Bioresour. Technol. 347, 126696 https://doi.org/10.1016/j.biortech.2022.126696.
Shahab, R.L., Luterbacher, J.S., Brethauer, S., Studer, M.H., 2018. Consolidated bioprocessing of lignocellulosic biomass to lactic acid by a synthetic fungal-bacterial consortium. Biotechnol. Bioeng. 115, 1207–1215. https://doi.org/10.1002/bit.26541.
Singhania, R.S., Patel, A.K., Singh, A., Haldar, D., Soam, S., Chen, C.-W., Tsai, M.-L., Dong, C.-D., 2022. Consolidated bioprocessing of Lignocellulosic biomass: Technological advances and challenges. Bioresour. Technol. 354, 127153 https://doi.org/10.1016/j.biortech.2022.127153.
Sung Su, Y., Nam, K., 2010. Pharmaceutical composition for treating or preventing sepsis or septic shock containing isoeugenol or derivative thereof as an active ingredient. South Korea. KR-20120004700-A.
Tramontina, R., Galman, J.L., Parmeggiani, F., Derrington, S.R., Bugg, T.D.H., Turner, N.J., Squina, F.M., Dixon, N., 2020. Consolidated production of coniferol and other high-value aromatic alcohols directly from lignocellulosic biomass. Green Chem. 22, 144–152. https://doi.org/10.1039/c9gc02359c.
Tramontina, R., Ciancaglini, I., Roman, E.K.B., Chacón, M.G., Corrêa, T.L.R., Dixon, N., Bugg, T.D.H., Squina, F.M., 2023. Sustainable biosynthetic pathways to value-added bioproducts from hydroxycinnamic acids. Appl. Microbiol. Biotechnol. 107, 4165–4185. https://doi.org/10.1007/s00253-023-12571-8.
Tran, N.P., Gury, J., Dartois, V., Nguyen, T.K.C., Seraut, H., Barthelmebs, L., Gervais, P., Cavin, J-F., 2008. Phenolic acid-mediated regulation of the *padC* gene, encoding the phenolic acid decarboxylase of *Bacillus subtilis*. J. Bacteriol. 190, 3213–3224. https://doi.org/10.1128/JB.01936-07.
Wang, Y.L., Wang, W.K., Wu, Q.C., Yang, H.J., 2022. The release and catabolism of ferulic acid in plant cell wall by rumen microbes: A review. Anim. Nutr. 9, 335–344. https://doi.org/10.1016/j.aninu.2022.02.003.
Wang, C., Zheng, P., Chen, P., 2019. Construction of synthetic pathways for raspberry ketone production in engineered *Escherichia coli*. Appl. Microbiol. Biotechnol. 3715–3725 https://doi.org/10.1007/s00253-019-09748-5.
Wei, Z., Zeng, G., Huang, F., Kosa, M., Huang, D., Ragauskas, A.J., 2015. Bioconversion of oxygen-pretreated Kraft lignin to microbial lipid with oleaginous *Rhodococcus opacus* DSM 1069. Green Chem. 17, 2784–2789. https://doi.org/10.1039/c5gc00422e.
Zhang, H., Wang, X., 2016. Modular co-culture engineering, a new approach for metabolic engineering. Metab. Eng. 37, 114–121. https://doi.org/10.1016/j.ymben.2016.05.007.
Zoghlami, A., Paës, G., 2019. Lignocellulosic Biomass: Understanding Recalcitrance and Predicting Hydrolysis. Front. Chem. 7 https://doi.org/10.3389/fchem.2019.00874.